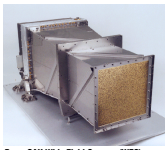

*Beppo*SAX Wide Field Camera (WFC)

Latest Results Comparing Prompt Emission from X-ray Flashes and Gamma-Ray Bursts

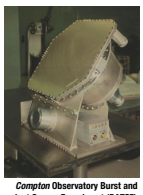

Compton Observatory Burst and Transient Source Experiment (BATSE)

R. Marc Kippen[1], **Peter M. Woods**[2], **Jean J. M. in 't Zand**[3,4], **John Heise**[4], **Robert D. Preece**[2], **Michael S. Briggs**[2]

[1] *Los Alamos National Laboratory, Los Alamos, NM, USA*
[2] *National Space Science and Technology Center, Huntsville, AL, USA*
[3] *Astronomical Institute, Utrecht University, Utrecht, The Netherlands*
[4] *SRON National Institute for Space Research, Utrecht, The Netherlands*

ABSTRACT

The final year of the *Beppo*SAX mission provided a much needed clue as to the nature of X-ray flashes. The detection of afterglow counterparts and their underlying hosts provides strong evidence that X-ray flashes and gamma-ray bursts originate from similar sources in cosmologically distant galaxies. These new observations support results that the prompt emission from X-ray flashes is quantitatively similar to that of classical gamma-ray bursts. Using the best wide-band observations that are available, we present the latest results in our on-going effort to quantify the similarities and differences in the prompt emission characteristics.

Introduction

The revolution in gamma-ray burst (GRB) astronomy prompted by the discovery of multiwavelength afterglow counterparts has brought tremendous progress in understanding the nature of burst progenitors, their surrounding environments, and host galaxies. Understanding of the mechanisms giving rise to the *prompt* burst emission itself, however, is comparatively confused despite a large amount of observational data. In this realm, one of the keys to better understanding lies in the identification of extreme characteristics that differ from those of the bulk ensemble, and can more severely constrain burst emission models. The goal of this paper is to investigate one such revealing characteristic — the lower energy form of the GRB emission process — by comparing prompt GRB properties to those of the so-called X-ray flashes [1] that could be a related phenomenon. We build on preliminary work [1,2,3] to quantitatively compare prompt emission from X-ray flashes (XRFs) and "traditional" GRBs. The analysis is based on a sample of XRFs that were selected based on *Beppo*SAX Wide Field Camera (WFC; 2–26 keV) X-ray observations, but also detected in 20-300 keV gamma rays through an off-line scan of BATSE data.

Table 1. *GRB-like WFC Transient Observation Summary 21-Apr-91 to 26-May-00*

WFC/GRBM Class	WFC Detections	Observable with BATSE	BATSE Triggers	BATSE Off-line Detect.
GRB	32	21	18	21
XRF	15	9	0	9
Questionable	7	4	0	4
Total	54	34	18	34

Observations

Our test sample is based on the events identified, selected, and "classified" using the *Beppo*SAX WFC and GRBM instruments. In this scheme, XRFs are differentiated from GRBs based on the lack of GRBM (40-400 keV) detection. Using simultaneous BATSE observations we can reveal wide-band spectral properties and make a more quantitative comparison between XRFs and "traditional" GRBs.

Apart from observational outages, the WFC and BATSE instruments operated simultaneously for 3.8 years, ending with the termination of BATSE science operations on 2000 May 26. For all of the GRB-like transient events detected by WFC, we performed an off-line search of the >20 keV BATSE data. Results of the search are listed in Table 1. Note that not all events were observable with BATSE due to data gaps and Earth occultations. The result is that all GRB-like WFC events that were observable with BATSE were detected with $\geq 5\sigma$ in the off-line search. This list includes four questionable events, three of which are likely long-duration GRBs (~1000 s), and one is likely a Type I X-ray burst. These questionable events are excluded from further analysis. For the remaining 21 GRB and 9 XRF (see Fig. 1) we have a complete set of WFC+BATSE data to use in comparing XRF and GRB properties.

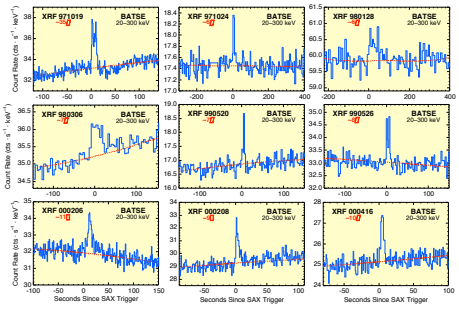

Fig. 1. *BATSE lightcurves for the 9 WFC XRF events observable with BATSE. Dashed lines indicate background model.*

Spectral Analysis

For each of the 30 XRF and GRB events we computed standard parameters (peak flux, fluence, and duration) using the same processes developed for the BATSE GRB catalogs. Furthermore, the WFC and BATSE data were used to jointly estimate the time-averaged 2 keV to 2 MeV spectrum of each event. Four separate spectral models were used in this process: black body (BB), power law (PL), power law times exponential (COMP), and Band's GRB function. Fitting results are listed in Table 2, and XRF spectra for the Band model are shown in Figure 2.

Based on the chi-squared values for the various models, we make the following conclusions. First, only one event is consistent with the BB model. This event is suspected to be a Type I X-ray burst.

Table 2. JOINT SPECTRAL FITTING RESULTS

Event Name	Data Pts.	Best-fit χ^2_ν BB	PLaw	Comp	Band	Best-fit Band Model Parameters* Amplitude[1]	E_{peak} (keV)	α	β
XRF 971019	40	237	206	48	47	39.40 ± 24.00	18.7 ± 0.8	-0.98 ± 0.18	-3.86 ± 0.36
XRF 971024	40	175	67	58	46	6780.00 ± 51100.00	5.9 ± 1.9	-0.44 ± 1.79	-2.01 ± 0.05
XRF 980128	40	110	48	30	29	0.91 ± 0.52	57.5 ± 17.5	-1.15 ± 0.18	-2.62 ± 0.73
XRF 980306	40	58	26	22	22	0.58 ± 0.46	49.2 ± 29.5	-1.36 ± 0.24	-2.36 ± 0.78
XRF 990520	40	95	44	22	22	4.64 ± 2.99	26.0 ± 3.2	-1.27 ± 0.20	-3.94 ± 2.89
XRF 990526	40	76	39	38	38	0.30 ± 0.19	14.7 ± 13.8	-1.89 ± 0.19	-5.0
XRF 000206	40	228	55	33	34	1.08 ± 0.27	38.2 ± 5.4	-1.64 ± 0.08	-5.0
XRF 000208	40	97	36	29	30	0.43 ± 0.18	86.8 ± 36.1	-1.39 ± 0.14	-3.05 ± 4.59
XRF 000416	40	101	46	41	43	1.31 ± 5.06	1.6 ± 6.6	-1.86 ± 0.92	-2.51 ± 0.11
GRB 960720	40	263	90	57	57	2.47 ± 0.19	659.3 ± 249.0	-1.28 ± 0.05	-5.0
GRB 970111	40	8655	26630	101	100	67.00 ± 1.02	160.2 ± 1.1	-0.62 ± 0.01	-4.79 ± 0.94
GRB 970508	40	549	35	35	35	1.12 ± 0.05	5000.0	-1.66 ± 0.02	-5.0
GRB 971214	40	516	705	32	29	7.11 ± 0.47	198.6 ± 11.0	-0.82 ± 0.06	-2.74 ± 0.37
GRB 971227	40	156	1080	26	26	50.20 ± 6.35	77.4 ± 2.3	-0.38 ± 0.08	-4.57 ± 2.00
GRB 980109	40	488	504	51	33	8.58 ± 0.89	114.1 ± 8.4	-0.93 ± 0.05	-2.25 ± 0.11
GRB 980326	40	246	481	58	52	32.30 ± 6.21	51.1 ± 3.0	-1.00 ± 0.09	-2.90 ± 0.17
GRB 980329	40	7151	4608	232	54	25.10 ± 0.67	216.5 ± 5.3	-0.84 ± 0.02	-2.17 ± 0.03
GRB 980425	40	421	190	43	43	4.72 ± 0.31	130.1 ± 10.4	-1.45 ± 0.04	-5.0
GRB 980519	40	2899	506	45	45	7.55 ± 0.22	239.6 ± 15.6	-1.31 ± 0.01	-4.00 ± 8.91
GRB 980613	40	138	56	47	45	1.46 ± 1.51	72.4 ± 66.8	-1.14 ± 0.33	-1.86 ± 0.13
GRB 990123	39	41971	26980	398	390	26.30 ± 0.12	642.3 ± 9.1	-0.88 ± 0.00	-2.89 ± 0.18
GRB 990510	40	3487	1225	57	33	8.80 ± 0.33	130.9 ± 5.7	-1.27 ± 0.02	-2.41 ± 0.09
GRB 990625	40	235	50	35	32	2.23 ± 0.93	55.9 ± 21.6	-1.50 ± 0.13	-2.24 ± 0.21
GRB 990705	38	6310	7404	98	62	34.90 ± 0.61	313.6 ± 6.2	-0.64 ± 0.02	-2.70 ± 0.10
GRB 990806	40	505	132	36	33	3.60 ± 0.31	180.3 ± 28.8	-1.34 ± 0.04	-2.17 ± 0.22
GRB 990907	40	393	158	47	46	3.14 ± 0.39	183.5 ± 29.2	-1.03 ± 0.05	-2.72 ± 1.17
GRB 991014	40	179	247	42	38	12.00 ± 2.04	97.9 ± 9.7	-0.96 ± 0.09	-2.31 ± 0.75
GRB 991105	40	312	134	41	33	5.90 ± 3.03	57.1 ± 16.4	-1.01 ± 0.16	-2.05 ± 0.07
GRB 000210	38	13066	5924	82	44	26.70 ± 0.28	414.8 ± 9.9	-1.01 ± 0.01	-2.44 ± 0.07
GRB 000424	40	514	169	50	37	4.92 ± 0.79	162.8 ± 36.4	-1.04 ± 0.07	-1.73 ± 0.05
GRB? 970111b	40	372	43	40	27	95.90 ± 416.00	7.1 ± 3.3	-0.39 ± 1.03	-1.70 ± 0.03
GRB? 981018	40	865	63	35	28	3.66 ± 3.28	45.2 ± 22.0	-1.06 ± 0.27	-1.95 ± 0.07
GRB? 990413	40	157	52	43	31	129.00 ± 547.00	15.6 ± 7.3	0.57 ± 1.17	-1.91 ± 0.17
XRB? 991106	40	31	47	29	29	519.00 ± 1890.00	9.6 ± 2.4	0.10 ± 0.96	-5.0

*Missing uncertainty indicates parameter value is at limit of allowed range.
[1] $\times 10^{-4}$ ph · cm^{-2} · s^{-1} · keV^{-1}

Second, for most GRB events (19 of 21) and three of the XRF events a single PL model can be rejected with good confidence. This is typical of GRBs, which usually have strongly curved (i.e., non power-law) spectra. Finally, the change in chi-squared from a power law to a COMP or Band model is statistically significant for most of the GRB and XRF events. This is an important indication that curved spectra are favored for XRFs just as they are for traditional GRBs.

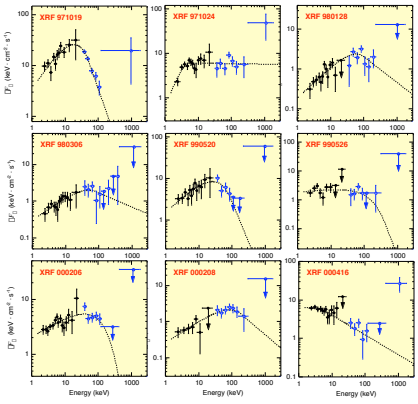

Fig. 2. *Jointly fit WFC+BATSE spectra of 9 XRFs using Band's GRB spectral model.*

XRFs vs. Bright GRBs

To compare the spectral properties of XRFs to those of bright GRBs we use the 21 WFC-selected GRBs and the Preece et al. (2000) catalog of 156 bright BATSE GRBs [BBG; 4]. Figure 3 compares the distributions of Band-model spectral parameters for the three event samples (similar results were obtained with the COMP model).

We use the Kolmogorov-Smirnov test on unbinned data to compare the different distributions. Statistical significance of observed deviations between distributions is evaluated through Monte Carlo simulations that account for the sample sizes as well as the measured statistical uncertainties in spectral parameters. Results are shown in Table 3. The Alpha and Beta parameters are marginally consistent between XRF and GRB, but XRFs have significantly lower E_{peak}.

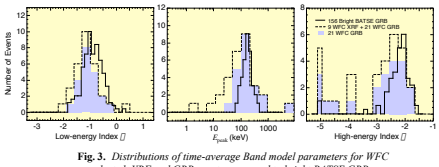

Fig. 3. *Distributions of time-average Band model parameters for WFC selected XRF and GRB events compared to bright BATSE GRBs.*

Table 3.
BRIGHT-GRB SPECTRAL PARAMETER COMPARISON

Samples Compared	Probability (D_{KS} > observed) α	E_{peak}	β
XRF+GRB vs. BBG	$2 \cdot 10^{-2}$	$7 \cdot 10^{-4}$	$1 \cdot 10^{-1}$
XRF vs. BBG	$1 \cdot 10^{-2}$	$2 \cdot 10^{-7}$	$1 \cdot 10^{-1}$
GRB vs. BBG	$8 \cdot 10^{-2}$	$6 \cdot 10^{-1}$	$2 \cdot 10^{-1}$
XRF vs. GRB	$2 \cdot 10^{-1}$	$2 \cdot 10^{-4}$	$8 \cdot 10^{-1}$

XRFs vs. Dim GRBs

The above bright burst comparison ignores the known GRB hardness–intensity correlation. It is important to compare XRFs to weak GRBs that have similar (gamma-ray) brightness. To do this we use the Mallozzi et al. (1998) sample of 623 BATSE bursts that were fit using the Band spectral model [MAL; 5]. Figure 4 compares these bursts with the WFC-selected events. The hardness–intensity correlation is evident in WFC GRBs and MAL GRBs.

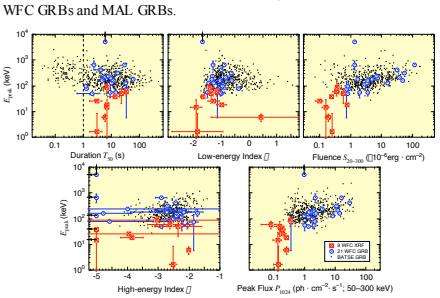

Fig. 4. *Time-average Band-model parameters of WFC-selected events compared to weak BATSE GRBs from [5]. First plot include short and long bursts. Other plots include only long (T50 > 1 s) bursts.*

To compare XRFs and dim GRBs we first modeled the hardness-intensity (E_{peak} vs. peak flux) correlation using a power-law fit to binned GRB data (including statistical uncertainties). The power-law was then extrapolated into the intensity regime of the XRFs (see Figure 5) assuming various models for the GRB intensity (Log$N$–Log$P$) distribution. Finally, the K-S test was used to compare the unbinned XRF data to the extrapolated GRB E_{peak} distribution. This analysis indicates that (within sizable uncertainties) XRFs and extrapolated dim WFC GRBs are statistically consistent, with chance K-S probability $P_{KS} \sim 0.2$–0.4 (depending on the choice of Log$N$–Log$P$). The extrapolated BATSE GRBs, however, have significantly larger E_{peak} than XRFs.

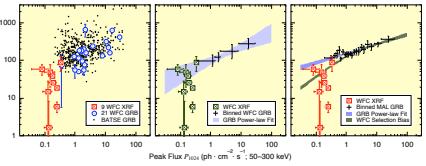

Fig. 5. *Long-duration GRB hardness-intensity data (left) binned and fit to a power law (center). The rightmost plot shows BATSE GRB data [5; MAL]. The brown curve indicates the effect of a simulated WFC selection bias on the power-law correlation.*

The above comparison ignores selection biases between WFC and BATSE samples. Starting with the BATSE power-law fit, we simulated the effect of the WFC selection bias assuming (1) Alpha and Beta are independent of burst intensity and described by the BBG distribution, (2) random locations over the WFC field of view, and (3) the approximate WFC trigger criteria. The effect of this simulated bias on the power-law hardness–intensity correlation is indicated on the right-most plot in Figure 5. Including this bias, the E_{peak} distribution of XRFs and extrapolated BATSE-selected dim GRBs are statistically consistent, with $P_{KS} \sim 0.1$ (depending on the choice of Log$N$–Log$P$).

Conclusion

While XRF-like events have been detected by *Ginga* in the past and HETE-II at present, the WFC+BATSE sample offers the greatest broad-band sensitivity. The nine jointly observed XRFs therefore represent a unique resource for comparing prompt XRF and GRB behavior.

Our results indicate that the prompt, broad-band emission from XRFs is quantitatively consistent with that expected from weak, long-duration, traditional GRBs. Combined with their similar temporal properties, this strongly suggests that XRFs and long GRBs are produced by a continuous variation the same phenomenon. Furthermore, XRFs are the majority component (>50%) of the combined XRF+GRB population when selection biases are included.

References

[1] Heise, J., in 't Zand, J., Kippen, R. M., & Woods, P. M. 2001, in ESO Astrophysics Symposia, Gamma-Ray Bursts in the Afterglow Era, ed. E. Costa, F. Frontera, & J. Hjorth (Berlin: Springer), 16

[2] Kippen, R. M., Woods, P.~M., Heise, J., et al. 2001, in ESO Astrophysics Symposia, Gamma-Ray Bursts in the Afterglow Era, ed. E. Costa, F. Frontera, & J. Hjorth (Berlin: Springer), 22

[3] Kippen, R. M., Woods, P. M., Heise, J., et al. 2003, in AIP Conf. Proc. 662, Gamma-Ray Burst and Afterglow Astronomy 2001, ed. G. R. Ricker & R. K. Vanderspek (New York: AIP), 244

[4] Preece, R. D., Briggs, M. S., Mallozzi, R. S., et al. 2000, ApJS, 126, 19

[5] Mallozzi, R. S., Pendleton, G. N., Paciesas, W. S., et al. 1998, in AIP Conf. Proc. 428, Gamma-Ray Bursts: 4th Huntsville Symp., ed. C. A. Meegan, R. D. Preece, & T. M. Koshut (New York: AIP), 273